Fault detection and isolation in system of multiple sources of energy using hierarchical Bayesian belief networks

Abbass Zein-Eddine, François Guérin, Iyad Zaarour, Abbas Hijazi, Dimitri Lefebvre

Fault Detection and Isolation in System of Multiple-Sources of Energy Using Hierarchical Bayesian Belief Networks

Abbass ZEIN EDDINE[1*], Francois GUERIN[2], Iyad ZAAROUR[3], Abbas HIJAZI[4], Dimitri LEFEBVRE[5]

[1*]SPIN-PMMG, Ecole Des Mines de Saint-Etienne, Saint-Etienne, France.
[2]Université Le Havre Normandie, ISEL, Le Havre, France.
[3]SAS, Ecole Des Mines de Saint-Etienne, Gardanne, France.
[4]Faculty of Science, Lebanese University, Beirut, Lebanon.
[5]Université Le Havre Normandie, GREAH, Le Havre, France.

*Corresponding author(s). E-mail(s): abbass.zeineddine@emse.fr;
Contributing authors: francois.guerin@univ-lehavre.fr; iyad.zaarour@emse.fr;
abhijaz@ul.edu.lb; dimitri.lefebvre@univ-lehavre.fr;

Abstract

Ensuring fault tolerance in Systems of Multiple-Sources of Energy (SMSE) is crucial for reliable operation. Detecting, localizing, and characterizing faults are essential tasks for system integrity. This paper presents a novel approach utilizing Hierarchical Bayesian Belief Networks (HBBNs) to identify and isolate open circuit faults in DC-DC power converters commonly employed in SMSE applications. Our method addresses the challenge of fault detection and isolation, significantly enhancing system reliability. In particular, we design a comprehensive system capable of detecting and isolating faults in a system of multiple DC-DC converters, leveraging the interpretability and efficiency of HBBNs. We also utilize measurements from other converters to detect and isolate faults in a single converter, enabling efficient fault management. Our approach utilizes regularly monitored variables of the system, eliminating the need for additional sensors, thereby reducing complexity and cost. Additionally, we generalize HBBNs to be adaptable to any number of converters, providing scalability and flexibility in fault detection and isolation. Notably, the interpretability and simplicity of HBBNs, with a small number of parameters compared to other data-driven methods such as neural networks, contribute to their effectiveness in fault management. Through extensive testing on simulated data generated via a developed state space model, our approach demonstrates its effectiveness in bolstering the robustness of DC-DC power converters against open circuit faults.

Keywords: Bayesian Belief Networks, DC-DC converters, System of Multiple Sources of Energy.

1 Introduction

In the contemporary era, electrical energy management has become ubiquitous fixtures in our daily lives. Electrical power forms the essence of every innovative creation. It serves as the fundamental force that sustains our existence. Consequently, there is an escalated demand for uninterrupted electrical energy, necessitating dependable electrical supply systems to meet consumers'

needs. Uninterrupted service requires fault-free systems that can anticipate and address any potential faults. To achieve this, the incorporation of a Fault Detection and Isolation (FDI) system is imperative. This system should promptly identify faults and subsequently discern the specific fault types. Among electrical engineering components, power converters have a pivotal role in the life cycle of electrical energy and are integral to almost all electrical engineering applications. In our study, we concentrate on such equipment, particularly the Zero-Voltage Switching (ZVS) full bridge isolated Buck converter. This converter holds significance in certain Systems of Multi Sources of Energy (SMSE) configurations, as depicted in Figure 1 [1]. It operates as a DC-DC converter managing the coordination and disconnection of energy sources on the DC-bus, aligning with load demands and available power.

The renewable energy systems under examination, shown in Figure 1, portray multisource setups. These systems are composed of diverse power sources and adaptable loads. These sources can provide power in either single-phase or three-phase modes through the utilization of an inverter. In our previous work we have proposed an FDI system for single DC-DC converters. [2] was the first attempt to use BBNs for DC-DC power converter FDI. We proposed a Bayesian Naive Classifier (BNC) model that predicts the probability of fault occurrence based on three measured variables, the measured average input current, the measured average output current and the measured output voltage. In [3] we improve the capabilities of Luenberger's observer by adding a BNC that uses the generated residuals to isolate the type of the occurring fault. Compared to our former work, our new contribution in this paper surpasses the problem of single DC-DC converter to the problem of Multiple DC-DC converters. We also consider the effect of the regulation loops that will try to bypass the side effects of the occurring fault. To solve this problem in such a complex system, we propose a two step solution. First, a dedicated HBBN is designed to detect the faulty converter. Then, another dedicated HBBN is used to isolate the occurring fault. This technique can be useful for the users and for the engineers in charge of repairing the faulty DC-DC converter. The contribution of our new paper can be summarized in the

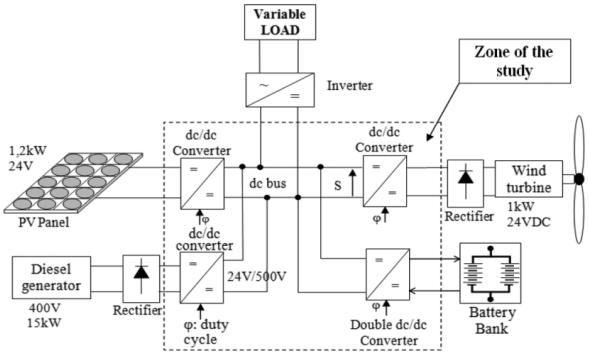

Fig. 1: Example of System of Multiple-Source of Energy (SMSE).

following points: (i) the design of complete system that is able to detect and isolate faults in a system of multiple DC-DC converters; (ii) the use of measurements from other converters to detect and isolate faults in one converter; (iii) the use of regularly monitored variables of the system, so no need to add new sensors; (iv) the generalization of HBBNs that can be extended and adapted to any number of converters. (v) The interpretability and the small number of parameters of the HBBNs used compared to other data driven methods such as neural networks. The subsequent sections of this article are structured as follows: Section 2 delves into the related literature, offering insights into the context of this study. Section 3 comprehensively outlines the studied system, encompassing its state space model. In Section 4, a succinct introduction to Bayesian Belief Networks (BBN) is provided. The proposed method, along with comprehensive experimental results, is elucidated in Section 5. Finally, Section 6 serves as the concluding segment, drawing together the various aspects discussed in this work.

2 LITERATURE REVIEW

2.1 Fault detection for energy systems

Numerous research endeavors have been dedicated to identifying and isolating faults within power converters. In [4], an innovative Fault Detection and Isolation (FDI) scheme was introduced for a quadratic boost converter. This approach enables the diagnosis of Open-Circuit Faults (OCF) and Short-Circuit Faults (SCF) affecting switches and

diodes. In this scenario, the fault characteristics were identified based on inductor voltages. To facilitate voltage measurements, an auxiliary winding was incorporated into the inductor's magnetic core. Additionally, the implementation of the FDI strategy required a logic circuit and a Pulse-Width Modulation (PWM) signal. Further research has proposed several schemes for diagnosing OCF and SCF in single-switch DC-DC converters [5], [6], [7]. For instance, [5], accurate prediction of the inductor current was enabled through the consideration of inductor current, input, and output voltages of the boost converter. Deviations between the predicted and measured inductor current facilitated the detection of switch faults. However, the sensitivity of this proposal to parametric uncertainties was noted due to threshold selection based on converter parameters. Reference [6] proposed a technique where switches and diodes OCF and SCF could be diagnosed. This involved the inclusion of diode voltage measurements and a logic circuit within the DC-DC converter. A comprehensive monitoring system encompassing switches and diodes OCF and SCF, switches and capacitores aging, and inductor interturn faults was presented in [7]. This scheme employed two electrical sensors and two temperature sensors for comprehensive fault detection. In another instance, [8] introduced a model-based FDI approach involving a sliding mode observer and residual generation applied to a three-cell power converter. Additionally, [9] formulated a set of residuals through a parity space algorithm based on a variable structure state-space model to detect sensor faults in ZVS full bridge isolated Buck converters. This endeavor was further expanded upon in [10] by integrating an extra measurement strategy reliant on a magnetic near-field probe. References [11] and [12] introduced model-based FDI approaches for diagnosing OCF and SCF in DC-DC boost converters. The paper [13] introduced a data-driven approach for fault detection, applicable to various types of DC-DC converters. The method involves statistical feature estimation through Gaussian process regression, specifically tailored for fault detection objectives. In recent investigations, Wang et al. [14] proposed an FDL scheme that capitalizes on the distinct patterns and elevated values of capacitor voltages in faulty submodule (SM) units, as opposed to healthy ones. By exploiting this knowledge, specific voltage signature signals are chosen, and waveforms composed of these signatures are reconstructed using signal synthesis techniques to accurately identify and locate faults. Additionally, data-driven strategies that incorporate machine learning models have been adopted to address the FDI challenge in power converters. Fahim et al. [15] introduced an unsupervised power converter fault detection and classification scheme based on sparse autoencoders. This method learns fault-specific features from unlabeled datasets.

In another vein, authors in [16] proposed an FDD framework that combines the strengths of the kernel principal component analysis (KPCA) model and the bidirectional long short-term memory (BiLSTM) classifier, particularly for wind energy converter systems. Analyzing the wavelet transform of power converter faults through effective machine learning techniques based on K nearest neighbors is discussed in [17]. Similarly, Sun et al. [18] employed neural networks to develop a fault recognition methodology utilizing continuous wavelet transform and convolutional neural network (CWT-CNN). This approach not only adaptively extracts features but also circumvents the complexity and subjectivity associated with manual feature extraction. Gandomi et al. [19] introduced an innovative deep learning approach for identifying and localizing faults in isolated DC-DC converters. Specifically targeting open-circuit faults in switches, this algorithm utilizes data-driven recursive discrete Fourier transform to derive feature vectors from repetitive primary voltage signals observed in both normal and faulty operation scenarios. Ultimately, a straightforward deep neural network model comprising 1D convolutional and dense layers is employed to effectively detect faulty switches within the converter.

2.2 Bayesian belief networks

Bayesian belief network is a probabilistic graphical model that represents a set of random variables and their conditional dependencies via a Directed Acyclic Graph (DAG). These graphical structures are used to represent knowledge about an uncertain domain [20] where each random variable of the modeled system is represented by a node, and these nodes are related to each other via arcs.

Those arcs represent the conditional dependencies between nodes which are often estimated by using known statistical and computational methods. Hence, BNs combine principles from graph theory, probability theory, computer science, and statistics [20]. They enable an effective representation and computation of the Joint Probability Distribution (JPD) over a set of random variables. Bayesian network has two components, the structure of a DAG in addition to their parameters. The parameters are expressed in a manner which is harmonious with a Markovian property, where the Conditional Probability Distribution (CPD) at each node depends only on its parents. For discrete Random Variables (RV), this conditional probability is often represented by a table, containing the probability of each RV value given all combinations of its parent's values. The joint distribution of a collection of variables can be determined uniquely by these local Conditional Probability Tables (CPTs) [20].

Bayesian Belief Networks (BBN) have garnered widespread adoption within the domain of fault detection and isolation [21], finding utility across diverse sectors. Notably, they have found application in energy systems, exemplified by their role in wind turbine fault detection [22], as well as their contribution to enhancing the fault detection capabilities of electrical power systems [2, 3, 23]. Moreover, the utilization of BBN extends to the realm of manufacturing systems. Their effectiveness has been observed in semiconductor manufacturing [23], where they aid in fault diagnosis, and in assembly systems [24], streamlining fault detection processes. In the realm of process systems, BBNs have been harnessed for fault detection and isolation purposes. Notable applications include their role in control loops [25] and assembly processes [26], where they contribute to improving the accuracy and efficiency of fault detection mechanisms. It is noteworthy that BBNs also find application in various other domains [27–29], showcasing their adaptability and significance across multiple fields.

Compared to other data drive methods, HBBN is designed based on the system variables and the dependency between those variables. This makes it an interpretable method, and thus we can interpret the results and understand the facts behind its output. HBBN also gives the possibility of integrating expert knowledge with data [30]. Another thing that makes HBBNs useful is their robustness to over-fitting compared to other methods [31]. In this work we investigate the effectiveness of using HBBN in the domain of FDI in SMSE.

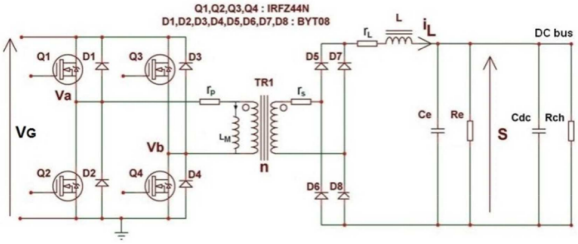

Fig. 2: ZVS full bridge isolated Buck converter structural diagram [2]

.

3 STUDIED SYSTEM

The schematic representation of the ZVS full bridge isolated Buck converter is depicted in Figure 2. These DC-DC converters encompass isolated Buck converter architecture with high-frequency transformer TR1, complemented by full bridge control involving Q1, Q2, Q3, and Q4 transistors. The implementation of Zero-Voltage Switching (ZVS) is achieved through a phase shift controller, such as the UC3879. The developed state space model can be found in [2].

These specific DC-DC converters find extensive applications in various renewable energy contexts [1]. Their utility is particularly prominent for managing energy transfer from sources to loads via a DC bus interface. The architecture proves advantageous in scenarios where multiple converters are requisite to meet load demands. These converters are interconnected on a shared DC bus and are manipulated through their duty cycle to align with a reference voltage. Consequently, control loops are responsible for regulating the duty cycle, a concept exemplified by the System of Multiple Sources of Energy illustrated in Figure 1.

The authors in [32] have developed an average state space model for several DC-DC converters coupled on a DC-bus, that depends on the duty cycle value $\varphi(t)$, controlled by the analog voltage control input.

Table 1: List of Symbols.

Variable	Symbol
Inductance current	I_L
Output voltage	S
Source voltage	V_G
Duty cycle	φ
Coil inductance	L
Coil resistance	r_L
Ratio of the HF transformer	N
Equivalent capacitance	C_{EQ}
Equivalent resistance	R_{EQ}

Let us define a multi-converter model by introducing the state vector $X_M = [I_{L_1}, ..., I_{L_n}, S]^T$, the control vector $U_M = [\varphi_1, ..., \varphi_n]^T$ and the output vector $X_M = [I_{L_1}, ..., I_{L_n}, S]^T$ where n is the number of the coupled converters. By neglecting the threshold voltage of the diodes (V_d), the resistance r_p and r_s of primary and secondary coils of the HF transformer, and the resistance r_{mos} of the MOSFETs. The following equations can be derived for every converter i:

$$L_i \dot{I_{L_i}} + r_{L_i} I_{L_i} = N.V_{G_i}\varphi_i - S, \tag{1}$$

Then

$$\dot{I_{L_i}} = \frac{N.V_{G_i}\varphi_i}{L_i} - \frac{r_{L_i} I_{L_i}}{L_i} - \frac{S}{L_i}, \tag{2}$$

And

$$C_{EQ}.\dot{S} = I_{L_1} + I_{L_2} + ... + I_{L_n} - \frac{S}{R_{EQ}}, \tag{3}$$

Then

$$\dot{S} = \frac{I_{L_1}}{C_{EQ}} + \frac{I_{L_2}}{C_{EQ}} + ... + \frac{I_{L_n}}{C_{EQ}} - \frac{S}{C_{EQ}R_{EQ}}, \tag{4}$$

The state space matrices (A_M, B_M, and C_M) are defined as:

$$A_M = \begin{bmatrix} \frac{-r_{L_1}}{L_1} & 0 & 0 & ... & 0 & \frac{-1}{L_1} \\ 0 & \frac{-r_{L_2}}{L_2} & 0 & ... & 0 & \frac{-1}{L_2} \\ 0 & ... & \ddots & ... & 0 & \frac{-1}{L_3} \\ \vdots & 0 & ... & \ddots & \vdots & \vdots \\ 0 & 0 & 0 & ... & \frac{-r_{Ln}}{L_n} & \frac{-1}{L_n} \\ \frac{1}{C_{EQ}} & \frac{1}{C_{EQ}} & \frac{1}{C_{EQ}} & \cdots & \frac{1}{C_{EQ}} & \frac{-1}{C_{EQ}R_{EQ}} \end{bmatrix}, \tag{5}$$

$$B_M = \begin{bmatrix} \frac{N.V_{G_1}}{L_1} & ... & 0 & 0 \\ 0 & \frac{N.V_{G_2}}{L_2} & ... & \vdots \\ \vdots & \vdots & \ddots & 0 \\ 0 & ... & 0 & \frac{N.V_{G_n}}{L_2} \\ 0 & ... & ... & 0 \end{bmatrix}, \tag{6}$$

$$C_M = I_{p+1}. \tag{7}$$

Table 1 gives the list of the symbols. Electrical malfunctions can manifest as short circuits, open circuits, or leakages. In our research, we focus on three distinct open circuit faults: MOSFET open circuit, diode open circuit, and coil open circuit. Typically, these open circuit faults are not inherently detrimental to the controllers and drivers of power MOSFETs, and they usually don't result in system shutdowns. However, there is a potential for these faults to trigger secondary issues in other system components [33].

In this paper we consider the three main open circuit faults that affect power converters. The open circuit MOSFET fault (f_1), the open circuit diode fault (f_2), and the open circuit coil fault (f_3). Those faults are studied individually, i.e., we did not take into consideration the simultaneous fault occurrence.

4 FDI USING HIERARCHICAL BBN IN SYSTEM OF MULTIPLE DC-DC CONVERTERS

The BBN structure is designed according to the considered problem and to the available variables that mostly represent the studied system. Thus, the complexity of the BBN structure increases whenever the system complexity and the problem complexity increases. However, the arcs between the nodes are constrained to the logical dependency and causality between the variables.
In an FDI problem, an important task is to select variables that really reflect the fault occurrence. Then, these variables are used to build-up the BBN structure.

4.1 Bayesian belief network structure and parameters

Hierarchical Bayesian Belief Network (HBBN) has no formal definition. On the one hand, HBBN refers to the generalization of standard BBN, defined over a structural data type [34]. On the other hand, it refers to a model with three or more levels of random variables [35]. HBBNs can represent knowledge at multiple levels of abstraction. Accordingly, they have been applied to many cognitive problems such as causal reasoning [36], vision [37], and decision making [38]. In our work, the HBBN is introduced to the domain of fault detection and isolation in power converters.

Our goal is to detect and isolate faults in systems of multi DC-DC converters which are performing together to satisfy the load. In contrast to our previous work [3, 39], the regulation loops are included in the considered system, [32] which make the task of detection and isolation more complex and should be performed in a very short time, the HBBN structure should be simplified as much as possible, but at the same time should respect the variables dependency. Therefore, to simplify the HBBN structure, the task is divided into two subtasks: (i) detect faulty converter; (ii) isolate the fault in the detected faulty converter. The first HBBN that aims to perform (i) will always run in parallel with the system while the second HBBN that aims to perform (ii) will run only when the first HBBN detects a fault.

4.1.1 Detecting the faulty converter

The DC-DC converters are controlled by regulation loops that modify their duty cycle (φ) value in order to satisfy the load demands and follow the reference voltage value [40]. The duty cycle of each DC-DC converter is modified according to the conditions (sources, loads ...) or the fault occurrence. Thus, the monitoring of the duty cycles in the system can help to detect the faulty converter. Another criterion that makes the duty cycle appropriate to be used for detection is the mode of modification that is the conditions under which the duty cycle is modified. In the case of the resource or load variation, the value of the duty cycle varies smoothly. While in the case of fault occurrence the variation is very sharp. This fact takes us to the idea of using the derivative that

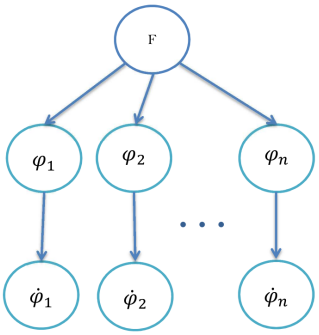

Fig. 3: General HBBN structure for faulty converter detection.

reflects the sharp deviation in the signal. Therefore two variables are chosen to detect the faulty converter, first the duty cycle and second the derivative of the duty cycle. In addition, another variable F that represents the system status, i.e. if any of the converters is faulty or it is a fault free case. F can take one of the following values $conv_f$ in case of fault free system or $conv_i$ where i is the identification of the faulty converter. The occurrence of the fault will lead to change in the duty cycle, and this change will lead to change in the derivative. In addition, mathematically, the derivative is derived from the signal, and thus the derivative of the duty cycle is affected by the signal. This means that in the HBBN structure there is an arc that connects the node representing φ to the node representing its derivative and this arc oriented toward the derivative node. Moreover, the node representing φ is also directly affected by the fault occurrence which leads to an arc oriented from the node representing the faulty converter identifier towards the φ node. This interpretation drives us to the general structure visualized in Figure 3, where node F stands for the system faulty state (fault free, or the identifier i of the faulty converter), φ is the duty cycle of converter i, $\dot{\varphi}_i$ is the duty cycle derivative of converter i and n is the number of converters.

4.1.2 Isolating the fault in the faulty converter

After detecting the faulty converter in the system, it is important to specify the type of the occurring fault. The models proposed in our previous work [39] and [3] were designed to detect and isolate faults in a single DC-DC converter and are based

on Bayesian Naive Classifiers (BNCs). Such BNC cannot fit in our new system for three reasons. First, in the BNC structure we did not consider the existence of the regulation loops, which will strongly affect the observations. In addition, using the BNC requires the collection of the output measurements of each converter used in the whole system, which makes it expensive. Moreover, a BNC should be implemented for each converter, but what we need here is a general form that is easy to expand when adding or removing any converter during the operation of SMSE. For these reasons another HBBN structure is specified. This structure should reflect in detail the DC-DC converters and the characteristic of the faults as much as possible in order to distinguish between the faults and have the ability to isolate the occurring fault. Thus each DC-DC converter is represented by a special node. This node mirrors the faulty status of the DC-DC converter according to the available observation. In addition as mentioned before the duty cycle reflects the fault occurrence which makes it helpful to isolate the occurring fault. Moreover, since the main affected variables during the fault occurrence are the output variables and since the average voltage on the DC-bus should follow a reference value which makes it unhelpful, the inductance current i.e. current provided to the load I_L is a good variable to be chosen for the isolation task.

According to the latter interpretation three node types are introduced to the HBBN structure: (i) the faulty status C_i (f_1, f_2 and f_3) of the converter i (ii) the duty cycle φ_i of the converter i; (iii) the inductance current I_{L_i} of the converter i. Those nodes are connected by arcs according to the dependency between them. In fact the occurrence of a fault in any converter will affect the duty cycle of all the coupled converters on the DC-bus. Therefore, each node C_i is connected to all the nodes φ_i via an arc pointing to the nodes φ_i. The change in φ_i will lead to a change in I_{L_i}, because the regulation loops will try to bypass and regulate the fault effects. Consequently, for each node φ_i an arc is add connecting φ_i by I_{L_i}, and this arc is oriented towards the I_{L_i} node as shown in Figure 4. Finally the structure is constructed according to the listed description. Figure 4 shows the general structure for a system of n DC-DC converters.

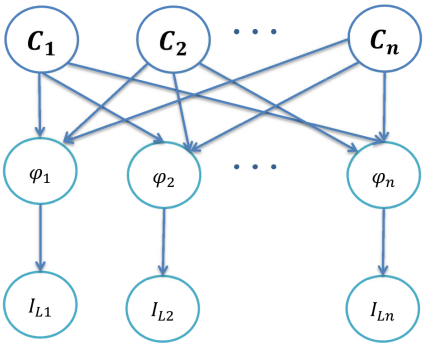

Fig. 4: General HBBN structure for fault isolation.

4.2 Simulation results

The suggested interpretation and methodology are verified and tested through simulated data generated by the state space model presented in Equations (5) to (7). We consider a system of two DC-DC converters. Equations (8) to (13) represent the state space model of the system with two DC-DC converters in the fault free case.

$$X_M = [I_{L1}, I_{L2}, S]^T, \tag{8}$$

$$U_M = [\varphi_1, \varphi_2]^T, \tag{9}$$

$$Y_M = [I_{L1}, I_{L2}, S]^T, \tag{10}$$

$$A_M = \begin{bmatrix} \frac{-r_{L1}}{L_1} & 0 & \frac{-1}{L_1} \\ 0 & \frac{-r_{L2}}{L_2} & \frac{-1}{L_2} \\ \frac{1}{C_{EQ}} & \frac{1}{C_{EQ}} & \frac{-1}{C_{EQ}.R_{EQ}} \end{bmatrix}, \tag{11}$$

$$B_M = \begin{bmatrix} \frac{N.V_{G1}}{L_1} & 0 \\ 0 & \frac{N.V_{G2}}{L_2} \\ 0 & 0 \end{bmatrix}, \tag{12}$$

$$C_M = I_2. \tag{13}$$

4.2.1 Fault modeling

In this case there are three faults to be modeled for each converter. Open circuit MOSFET fault (f_1) in converter 1 and converter 2, open circuit diode fault (f_2) in converter 1 and converter 2, and open circuit coil fault (f_3) in converter 1 and converter 2. Open circuit MOSFET fault and open circuit diode fault can be assimilated to control faults, so they are simulated by changing the control matrix. But due to the complexity of the system and the similarity of both fault effects which makes it difficult to simulate using the state space model in

Equations (5) to (7), both of them are simulated by dividing the value related to the duty cycle in the control matrix by 2 as shown in Equations (14) and (15) for converter 1 and converter 2 respectively. The open circuit coil is simulated by just making the value of r_L in the faulty converters go to infinity because during the open circuit coil the output current I_L goes to zero.

$$B_{M_{C_1}} = \begin{bmatrix} \frac{N.V_{G1}}{2L_1} & 0 \\ 0 & \frac{N.V_{G2}}{L_2} \\ 0 & 0 \end{bmatrix}, \tag{14}$$

$$B_{M_{C_2}} = \begin{bmatrix} \frac{N.V_{G1}}{L_1} & 0 \\ 0 & \frac{N.V_{G2}}{2L_2} \\ 0 & 0 \end{bmatrix}. \tag{15}$$

4.2.2 Data Collection

The main challenge to the proposed FDI method is to distinguish between the normal sources and load variation and the fault occurrence. Thus, several data sets are recorded each one corresponds to one of the open circuit faults and to one of the two DC-DC converters. In addition, some measurements are recorded for the normal sources and load variation case. Knowing that f_1 and f_2 are simulated the same way by dividing the value related to the duty cycle in the control matrix by 2, six dataset measurements are recorded. Each set is composed of seven variables: I_{L1}, I_{L2}, S, φ_1, φ_2, $\dot{\varphi_1}$, and $\dot{\varphi_2}$. The simulation is considered in sampled time with the sampling period $Te = 0.1ms$ according to a first order method, and faults are simulated starting from time $t = 5s$ to the end of simulation at time $t = 10s$. To structure the data collection process, let us define the following scenarios: *scenario* 1: simulating f_1 and f_2 in converter 1, *scenario* 2: simulating f_1 and f_2 in converter 2, *scenario* 3: simulating f_3 in converter 1, *scenario* 4: simulating f_3 in *converter* 2, *scenario* 5: simulating normal resource changes of converter 1, and *scenario* 6: simulating normal resource changes of converter 2. Figure 5 visualizes the variables I_{L1}, I_{L2}, S, φ_1, φ_2, $\dot{\varphi_1}$, and $\dot{\varphi_2}$ of the datasets of measurements related to converter 1. Figure 5 (a) stands for *scenario* 1, the regulation loops try to bypass the fault by increasing φ_1, but when the value of φ_1 becomes 1 and cannot increase

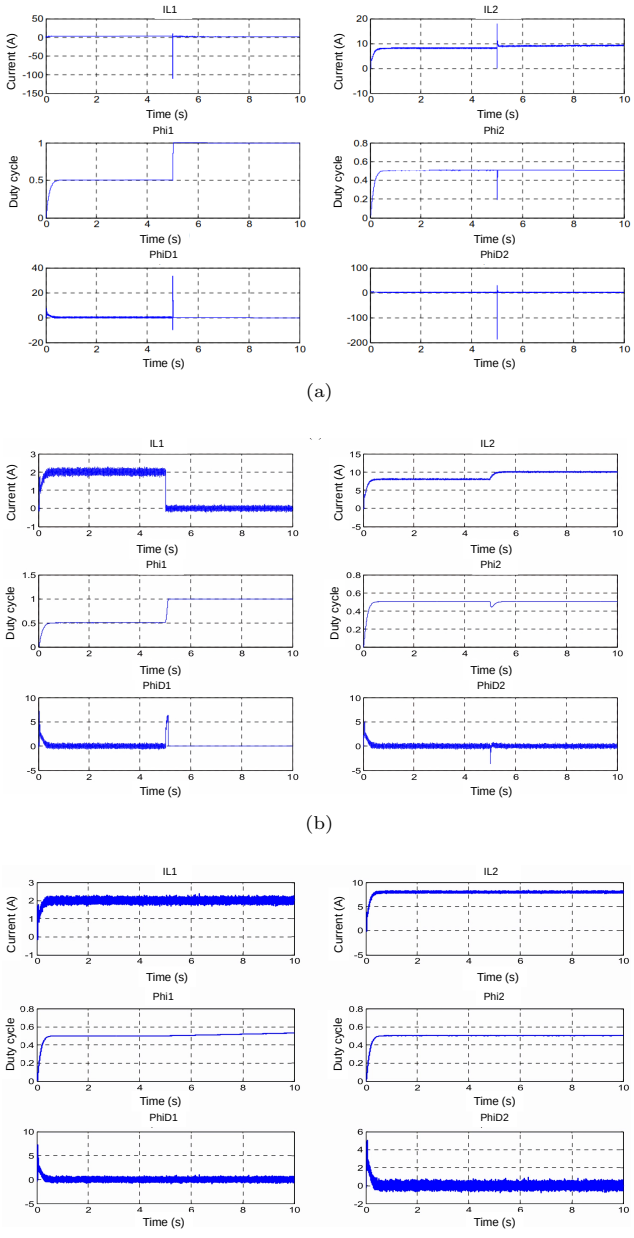

Fig. 5: Collected data: (a) fault 1 and 2 in converter 1; (b) fault 3 in converter 1; (c) normal resource changes for converter 1.

more, the value of I_{L2} increases to keep the value of the voltage on the DC-bus equal to the reference value ($300V$ in our case study). The sudden change in φ_1 value is captured by $\dot{\varphi_1}$ represented in Figure 5 and entitled as phiD1.

The same process is repeated in Figure 5 (b) which shows *scenario* 3. The normal variation in sources of converter 1 (*scenario* 5) is shown in Figure 5 (c). It shows that the normal variations do not lead to any significant changes in $\dot{\varphi_1}$ (Figure 5 a,b,c, bottom, left). The same happens for converter 2. We can also notice in Figure 5, that φ_2 is temporally affected for a few milliseconds before it goes back to its initial value. This weak effect is well represented in the CPTs calculated in the training phase of the HBBN, and is shown in the proposed results.

4.2.3 Faulty DC-DC converter detection

The collected data that describes the system in several situations are treated offline. First the data is quantized and binned [41]. Then a class value is given for each data point. In 10 seconds and with $Te = 0.1ms$, each dataset is formed of 105 data points. Thus each of these data points is labeled by a class value, which can equal to $conv_1$ if converter 1 is faulty, $conv_2$ if converter 2 is faulty and $conv_f$ if none of the DC-DC converters is faulty. After data cleaning and data preparation, the same training algorithm followed in "training phase" of the previously presented HBBNs is used.
The training phase will find the CPDs and fill in the CPTs. For demonstration, Fig. 6 shows the CPD of the node φ_1 given its parents, i.e., $P(\varphi_1/F)$ in the detection HBBN. It is clear that there exist different distributions: one for the fault-free case, one for the $f1$ or $f2$ case, and one for the $f3$ case. Fig. 7 represents $P(\varphi_1/C1, C2)$ in the isolation HBBN. In this case, φ_1 has two parent nodes, $C1$ and $C2$. It is important to note that in the CPT of φ_1, we will have columns that are not considered in our study, i.e., the existence of multiple faults simultaneously. One can see that those cases are represented as a straight line in the figure. Fig. 8 illustrates the CPD of the I_{L1} node in the isolation HBBN. The 3D plot shows that the CPT is a parsed matrix, which is essential for real-time applications.

Given the time span between the occurrence of a fault and the point at which regulation loops bypass the fault (when the DC-bus voltage returns to its reference value), which varies from $88ms$ to $138ms$, it's evident that the range of observations reflecting fault effects lies between 880 and 1380 data points. To facilitate training and testing, a subset of the measurement datasets is extracted. This subset must consider the ratio of occurrences between fault-free and faulty cases. However, since the number of observations representing fault occurrences is much smaller than those for fault-free cases, the observations for the faulty case are duplicated. Therefore, from each

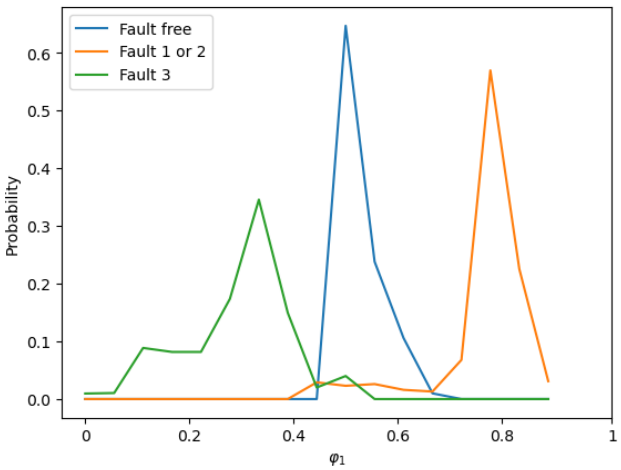

Fig. 6: Conditional Probability Distribution (CPD): Conditional Probability Distribution $P(\varphi_1/F)$

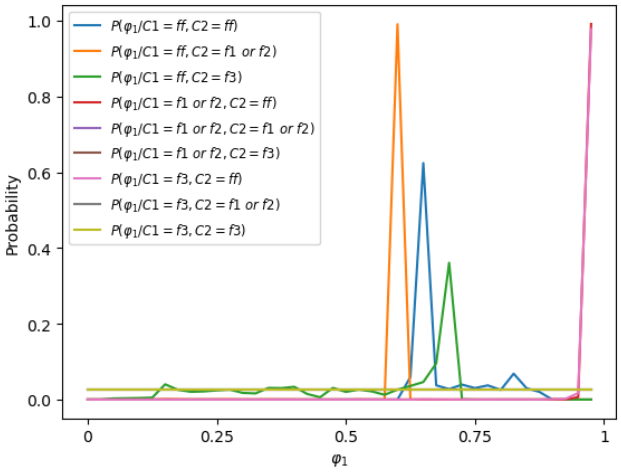

Fig. 7: Conditional Probability Distribution (CPD): Conditional Probability Distribution $P(\varphi_1/C1, C2)$

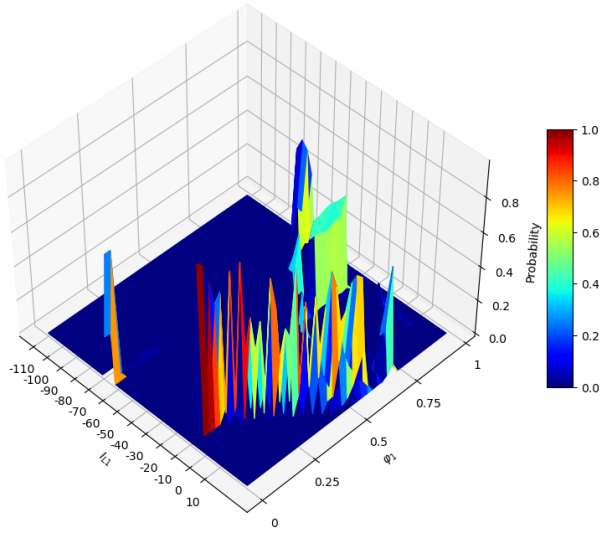

Fig. 8: Conditional Probability Distribution (CPD): Conditional Probability Distribution $P(I_{L1}/\varphi_1)$

simulated dataset of a faulty case, 1000 data points from the fault-free case are added, alongside the duplicated observations of the faulty case. Furthermore, a portion of the datasets reflecting normal resource variations is incorporated. Given that normal variations are simulated from $t = 5s$, 10000 data points are selected starting from that time stamp. In both fault and normal cases, each dataset contains 7 features: φ_1, $\dot{\varphi}_1$, φ_2, $\dot{\varphi}_2$, I_{L1},I_{L2}, and S. However, considering this HBBN models only the duty cycle of each DC-DC converter and its derivative, the columns corresponding to these variables, along with the class column, are retained.

Consider A_1 and A_4 as the sets of data points derived from the dataset simulating f_1 and f_2 in converters 1 and 2 respectively. Similarly, designate A_2 and A_5 as the sets of data points stemming from the dataset simulating f_3 in converters 1 and 2 respectively. Lastly, let A_3 and A_6 denote the sets of data points obtained from the dataset simulating normal source variations for converters 1 and 2 respectively.

Each of the datasets A_1, A_2, A_4, and A_5 is divided into two groups, each constituting 50% of the total records. Denote T_i as the 50% subset of the i^{th} dataset (A_i) utilized for training the HBBN, and V_i as the 50% subset of the i^{th} dataset (A_i) employed for validating the trained HBBN (Table 2). On the other hand, datasets A_3 and A_6 are exclusively used for testing purposes, aimed at evaluating the HBBN's capacity to differentiate between normal variations and faulty instances. Consequently, V_3 and V_6 align with A_3 and A_6 respectively. Subsequent to applying the Maximum Likelihood Estimation (MLE) algorithm [42], the initial HBBN designed to detect faulty converters is trained using the subsets T_i.

The faulty converter is detected based on the classification capabilities of the trained HBBN. For each set V_i, the observations $(\varphi_1,\varphi_2,\dot{\varphi}_1,\dot{\varphi}_2)$ are classified by the trained HBBN as $conv_1$, $conv_2$ or $conv_f$. Lying on the inference criteria of the HBBN and using the junction tree algorithm, at each time sample, the probability $P(F|\varphi_1, \varphi_2, \dot{\varphi}_1, \dot{\varphi}_2)$ is calculated. This step will return for each data point a vector $P(t)$ of three elements $P(t) = (P_{conv_1}, P_{conv_2}, P_{conv_f})$ where $P_{conv_1} = P(F = conv_1|\varphi_1, \varphi_2, \dot{\varphi}_1, \dot{\varphi}_2)$, $P_{conv_2} = P(F = conv_2|\varphi_1, \varphi_2, \dot{\varphi}_1, \dot{\varphi}_2)$, and $P_{conv_3} = P(F = conv_3|\varphi_1, \varphi_2, \dot{\varphi}_1, \dot{\varphi}_2)$.

The next step is to benefit from these probabilities. The class with maximum probability will be the estimated faulty case returned by the HBBN such that if $P_{conv_1} = max(P(t))$ then the classification is $conv_1$, if $P_{conv_2} = max(P(t))$ then the classification is $conv_2$, and if $P_{conv_f} = max(P(t))$ then the classification is $conv_f$. Let us denote C_i the HBBN classifications of the data points in the validation dataset V_i. In order to prevent false alarms the confidence (probability) of the classifications will be taken into consideration.

Figure 9 shows the HBBN classifications for the data in the validation sets (C_i sets). One can see that the classifications of the HBBN (green line) almost superpose with the actual case (dotted red line) in all the figures. This means that the HBBN has learned the faulty behavior of the system and is able to detect the faulty DC-DC converter just by knowing at least the value of the duty cycle of each DC-DC converter. Figures 9 (a) and (b) which belong to faults in converter 1 shows that the HBBN classifications after the fault occurrence are correct and the HBBN classification classifies the first point as a fault in converter one just after $0.1ms$ in (a) and $0.5ms$ in (b) which is a very short time comparing to duration before the regulation loops bypassed the fault effects ($88ms$ to $138ms$). Figures 9 (c) and

Table 2: Collected datasets and validation sets.

	Fault	Training Dataset		Validation Dataset	
		Name	Cardinality	Name	Cardinality
Converter 1	$f1$ and $f2$	T_1	941	V_1	941
	$f3$	T_2	1061	V_2	1061
	No fault	A_3	10000	A_3	10000
Converter 2	$f1$ and $f2$	T_4	941	V_4	941
	$f3$	T_5	1061	V_5	1061
	No fault	A_6	10000	A_6	10000

(d) represent the case of a fault in converter 2. The HBBN classifications in (c) detects the fault after a $0.1ms$ delay while in (d) after $0.2ms$ the HBBN classifies few points as converter 1 faulty which is not the case. Therefore the confidence of the HBBN classification is used, those values in our case are represented by the $P(t)$ vector. The average confidence of the few miss classified cases is equal to 41.7%. So, another condition is added to the detection process, that is, a detection alarm is ON whenever a point is classified as faulty (converter 1 faulty or converter 2 faulty) with confidence greater than 60% in order to insure the case and avoid false alarms. The classification shows that the HBBN is able to avoid the case of normal changes and classify it as no fault case. That is to say that, the HBBN is able to distinguish between the fault occurrence which leads to a sudden change in the system parameters, and the normal regularization resulting from the change in load demands which leads to a smooth change in the system parameters.

In fact, Figure 9 shows the efficiency of the proposed HBBN structure. Table 3 shows the total confusion matrix of the HBBN classifications. The total number of HBBN misclassifications is 20 points out of 24054 points. Based on the $P(t)$ vectors, the confidence of the classification in total is greater than 0.75. Therefore, in addition to the fact that none of the fault-free cases where misclassified, the final decision can be taken, such that whenever a point is classified as faulty (converter 1 faulty or converter 2 faulty), with a confidence note larger than 60%, a detection alarm is triggered. This process will limit the number of false alarms and wrong detections.

4.2.4 Fault isolation in the faulty DC-DC converter

During inference, if the first HBBN detects a fault in converter i then the node C_i in the isolation HBBN is going to be inferred (i.e, $P(C_i|observation)$). In this level the quantized data points will be treated offline. To train this isolation HBBN, we need to have labeled data that include the type of the occurring fault for each observation. Therefore we add two columns to our dataset. The first column C_1 is added to represent the faulty cases of converter 1, i.e. the values of the C_1 node. The second class column C_2 is added to represent the faulty cases of converter 2, i.e. the values of the C_2 node. The values of those two columns are f_f for fault free case or f_1, f_2 for fault 1 and fault 2 case, or f_3 for fault 3 case. Consequently, the data sets are similar to the ones used for detection, in addition to two columns for the classes C_1 and C_2.
Now let B_i be the part of the i^{th} dataset containing the data needed to train and test the second HBBN. Since this step comes after detecting the fault occurrence and the faulty converter, and since the role is to isolate the occurring fault, only the part after fault occurrence ($t = 5s$) is considered. This is done because the HBBN should be trained on the faults behavior, and it has no work to do with the fault free case. Note that the fault

Table 3: Confusion matrix for faulty DC-DC converter isolation.

Actual class / Classification	No fault	Converter 1 faulty	Converter 2 faulty
No fault	100%	1%	0.6%
Converter 1 faulty	0%	99%	0.4%
Converter 2 faulty	0%	0%	99%

free (f_f) case of node C_1 and C_2 mentioned before represents the case of converter 1 when converter 2 is faulty and the case of converter 2 when converter 2 is faulty respectively. This will lead us to 4 data sets each of them starting from $t = 5s$. Let B_1 the set of the data points considered from the first dataset simulating f_1 and f_2 in converter 1, B_2 the set of the data points considered from the first dataset simulating f_3 in converter 1, B_3 the set of the data points considered from the first dataset simulating f_1 and f_2 in converter 2, B_4 the set of the data points considered from the first dataset simulating f_3 in converter 2. The training process for this HBBN is the same for the previous ones, MLE algorithm is used. 50% of the records from each set B_i are used to complete this process. The remaining 50% are used for testing the trained HBBN as done in the previous HBBN structures. The aim of the validation is to see how much the HBBN learns the faults behavior's and if it is able to distinguish between faults depending on the observations. The classification of each observation gives us an idea about the ability of the HBBN to perform the isolation task. This classification is going to be the key of the isolation task.

Figure 10 shows the HBBN classification in green compared to the actual case in red. Those classifications specify the predicted fault type by the HBBN, and they will be used to make a decision about the occurring fault in the faulty converter. In order to isolate the fault several consecutive classifications are going to be considered, first to avoid false alarms and second to isolate the occurring fault. Those classifications in each subfigure (a), (b), (c), and (d) stand for the observations after fault detection. Figure 10 (a) and (b) shows the HBBN classifications generated by the second HBBN after detecting a fault in converter 1 by the first HBBN. In this case only the node C_1 is inferred and the results are plotted. Figure 10 (c) and (d) shows the HBBN classifications generated by the second HBBN after detecting a fault in converter 2 by the first HBBN. In this case only the node C_2 is inferred and the results are plotted. In the four subfigures several misclassifications occur especially in the first few observations, but one can see that in the first $50ms$ in all the figures the majority of classifications are correctly classified, and minor are the misclassifications. Thus taking about $50ms$ after each fault detection alarm is enough to isolate the correct fault.

In total the Figure 10 shows a small number of misclassifications. The confusion matrices in Table 4 and Table 5 show the number of misclassifications in each case and the percentage of accuracy. This accuracy reflects the high ability of isolation. As an average of the accuracy that can be derived from those tables one could say that the total accuracy of the system is above 97%.

Table 4: Confusion matrix for C_1 inference.

	f_1 and f_2	f_3
f_f	0%	0.01%
f_1 and f_2	99%	3.99%
f_3	1%	96%
Accuracy	99.5%	96.3%

Table 5: Confusion matrix for C_2 inference.

	f_1 and f_2	f_3
f_f	0%	0%
f_1 and f_2	99%	2.6%
f_3	1%	97.4%
Accuracy	99.1%	97.4%

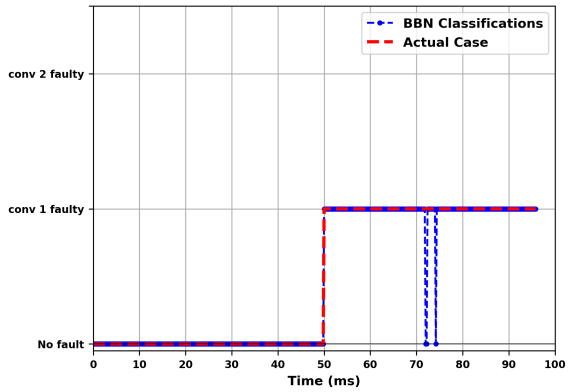

(a)

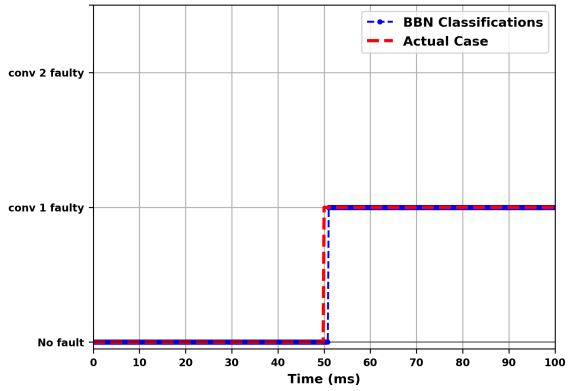

(b)

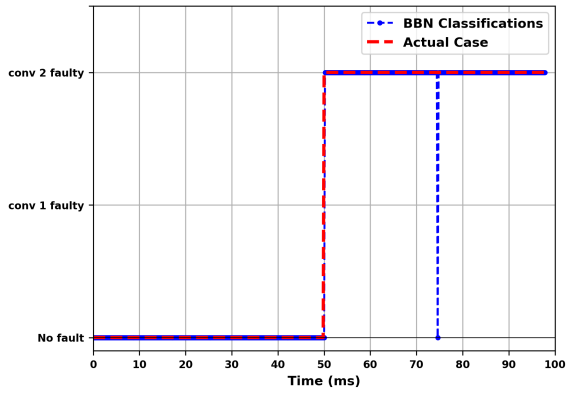

(c)

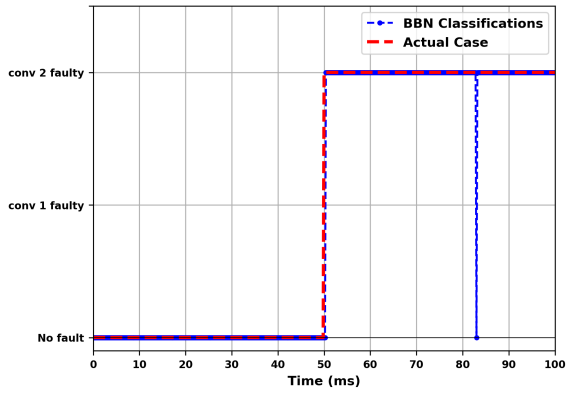

(d)

Fig. 9: HBBN classifications for detecting faulty converter: (a) when fault 1 and fault 2 in converter1 occurs; (b) when fault 3 in converter 1 occurs; (c) when fault 1 and fault 2 in converter3 occurs; (d) when fault 3 in converter 2 occurs;

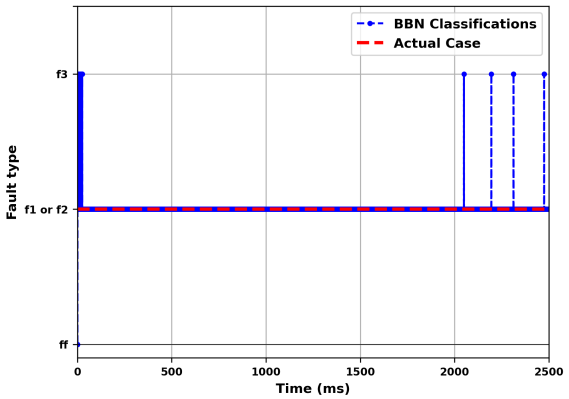

(a)

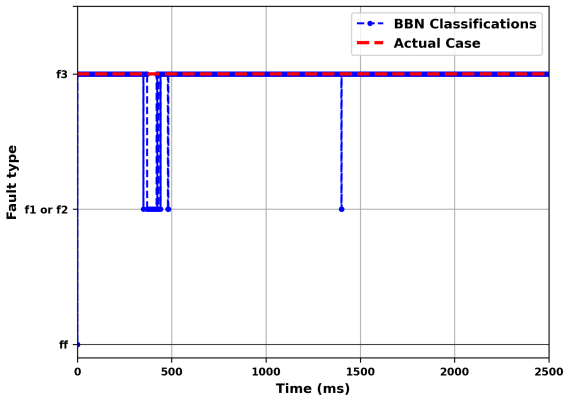

(b)

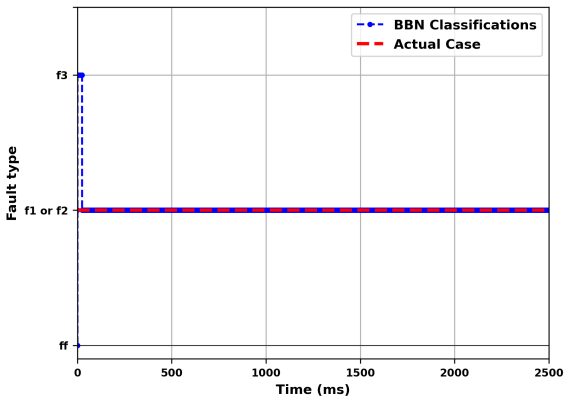

(c)

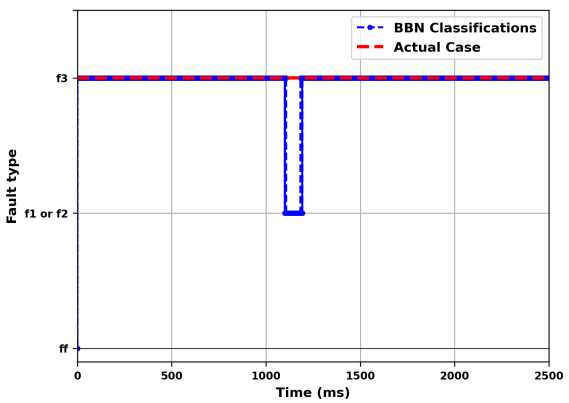

(d)

Fig. 10: HBBN classifications for isolate the occurring fault in the faulty converter: (a) when f_1 and f_2 in converter 1 occurs; (b) when f_3 in converter 1 occurs; (c) when f_1 and f_2 in converter 3 occurs; (d) when f_3 in converter 2 occurs.

5 CONCLUSION

This paper introduces a comprehensive approach for open circuit fault detection and isolation in multi-DC-DC converter systems, employing two specialized Hierarchical Bayesian Belief Networks (HBBNs). The first HBBN identifies the faulty converter, while the second isolates the fault type. Both HBBNs share a generalized structure. Rigorous testing on simulated data from a two-DC-DC converter system demonstrates the robustness of HBBNs in learning system behavior and efficiently categorizing observations for Fault Detection and Isolation (FDI). The decision from the first HBBN guides the inference process in the second, enhancing the potential of HBBNs for effective fault detection and isolation in complex multi-converter systems.
In future works, in order to deal with multiple types of faults, including scenarios where different faults may occur simultaneously, larger training data in various scenarios will be considered. Additional experiments with real data will be also pursued to validate the efficiency of the proposed method.

6 Declarations

Funding and/or Conflicts of interests/Competing interests
No conflicts of interest to declare

References

[1] Guérin, F. *et al.* Hybrid modeling for performance evaluation of multisource renewable energy systems. *IEEE transactions on automation science and engineering* **8**, 570–580 (2011).

[2] Eddine, A. Z., Zaarour, I., Guerin, F., Hijazi, A. & Lefebvre, D. Improving fault isolation in dc/dc converters based with bayesian belief networks. *IFAC-PapersOnLine* **49**, 303–308 (2016).

[3] Eddine, A. Z., Zaarour, I., Guerin, F., Hijazi, A. & Lefebvre, D. A comparative study about the effectiveness of observers and bayesian belief networks for the fault detection and isolation in power electronics. *Research Journal of Applied Sciences, Engineering and Technology* **14**, 10–28 (2017).

[4] Chen, L., Zhao, X. & Tang, S. X. Online fault diagnosis method for high-performance converters using inductor voltage polar signatures. *IEEE Access* **8**, 179778–179788 (2020).

[5] Pazouki, E., Sozer, Y. & De Abreu-Garcia, J. A. Fault diagnosis and fault-tolerant control operation of nonisolated dc–dc converters. *IEEE transactions on Industry Applications* **54**, 310–320 (2017).

[6] Givi, H., Farjah, E. & Ghanbari, T. Switch and diode fault diagnosis in nonisolated dc–dc converters using diode voltage signature. *IEEE Transactions on Industrial Electronics* **65**, 1606–1615 (2017).

[7] Givi, H., Farjah, E. & Ghanbari, T. A comprehensive monitoring system for online fault diagnosis and aging detection of non-isolated dc–dc converters' components. *IEEE Transactions on Power Electronics* **34**, 6858–6875 (2018).

[8] Meziane, H., Labarre, C., Lefteriu, S., Defoort, M. & Djemai, M. Fault detection and isolation for a multi-cellular converter based on sliding mode observer. *IFAC-PapersOnLine* **48**, 164–170 (2015).

[9] Guerin, F. & Lefebvre, D. Residual analysis for the diagnosis of hybrid electrical energy systems. *IFAC Proceedings Volumes* **42**, 1366–1371 (2009).

[10] Guerin, F., Labarre, C. & Lefebvre, D. Magnetic near-field measurement for fdi of zvs full bridge isolated buck converter 344–349 (2011).

[11] Espinoza Trejo, D. R., Bárcenas, E., Hernández Díez, J. E., Bossio, G. & Espinosa Pérez, G. Open-and short-circuit fault identification for a boost dc/dc converter in pv mppt systems. *Energies* **11**, 616 (2018).

[12] Espinoza Trejo, D. R., Taheri, S. & Pecina Sánchez, J. A. Switch fault diagnosis for boost dc–dc converters in photovoltaic mppt systems by using high-gain observers. *IET Power Electronics* **12**, 2793–2801 (2019).

[13] Jiang, Y., Yu, Y. & Peng, X. Online anomaly detection in dc/dc converters by statistical feature estimation using gpr and ga. *IEEE Transactions on Power Electronics* **35**, 10945–10957 (2020).

[14] Wang, H., Li, Y., Wijesekera, A., Kish, G. J. & Zhao, Q. Switch open-circuit fault detection and localization for modular multilevel converters based on signal synthesis. *IEEE Journal of Emerging and Selected Topics in Power Electronics* (2023).

[15] Fahim, S. R., Bhuiyan, E. A., Sarker, Y., Sarker, S. K. & Das, S. K. An unsupervised fault detection and classification scheme of power converters. *IEEE Sensors Letters* **5**, 1–4 (2021).

[16] Yahyaoui, Z. *et al.* Effective fault detection and diagnosis for power converters in wind turbine systems using kpca-based bilstm. *Energies* **15**, 6127 (2022).

[17] Hassan, M., Ali, Z., Sadiq, M., Su, C.-L. *et al.* Fault detection of power converters in shipboard microgrids 1–6 (2022).

[18] Sun, Q., Yu, X., Li, H., Peng, F. & Sun, G. Fault detection for power electronic converters based on continuous wavelet transform and convolution neural network. *Journal of Intelligent & Fuzzy Systems* **42**, 3537–3549 (2022).

[19] Gandomi, A. A., Kargar, M., Kargar, S., Parsa, L. & Corzine, K. Deep-learning-based fault detection and location method applied on isolated dc-dc converter 2245–2252 (2023).

[20] Ben-Gal, I. *Bayesian Networks* (John Wiley and Sons, 2007).

[21] Cai, B., Huang, L. & Xie, M. Bayesian networks in fault diagnosis. *IEEE Transactions on industrial informatics* **13**, 2227–2240 (2017).

[22] de Bessa, I. V., Palhares, R. M., D'Angelo, M. F. S. V. & Chaves Filho, J. E. Data-driven fault detection and isolation scheme for a wind turbine benchmark. *Renewable Energy* **87**, 634–645 (2016).

[23] Mengshoel, O. J. *et al.* Probabilistic model-based diagnosis: An electrical power system case study. *IEEE Transactions on Systems, Man, and Cybernetics-Part A: Systems and Humans* **40**, 874–885 (2010).

[24] Sayed, M. S. & Lohse, N. Ontology-driven generation of bayesian diagnostic models for assembly systems. *The International Journal of Advanced Manufacturing Technology* **74**, 1033–1052 (2014).

[25] Qi, F. & Huang, B. Bayesian methods for control loop diagnosis in the presence of temporal dependent evidences. *Automatica* **47**, 1349–1356 (2011).

[26] Liu, Y. & Jin, S. Application of bayesian networks for diagnostics in the assembly process by considering small measurement data sets. *The International Journal of Advanced Manufacturing Technology* **65**, 1229–1237 (2013).

[27] Bartram, G. W. *System health diagnosis and prognosis using dynamic Bayesian networks.* Ph.D. thesis (2013).

[28] Bennacer, L., Amirat, Y., Chibani, A., Mellouk, A. & Ciavaglia, L. Self-diagnosis technique for virtual private networks combining bayesian networks and case-based reasoning. *IEEE Transactions on Automation Science and Engineering* **12**, 354–366 (2014).

[29] Carrera, Á., Iglesias, C. A., García-Algarra, J. & Kolařík, D. A real-life application of multi-agent systems for fault diagnosis in the provision of an internet business service. *Journal of Network and Computer Applications* **37**, 146–154 (2014).

[30] Constantinou, A. C., Fenton, N. & Neil, M. Integrating expert knowledge with

data in bayesian networks: Preserving data-driven expectations when the expert variables remain unobserved. *Expert systems with applications* **56**, 197–208 (2016).

[31] Kelly, R. S. *et al.* Partial least squares discriminant analysis and bayesian networks for metabolomic prediction of childhood asthma. *Metabolites* **8**, 68 (2018).

[32] Guerin, F., Lefebvre, D. & Loisel, V. Supervisory control design for systems of multiple sources of energy. *Control Engineering Practice* **20**, 1310–1324 (2012).

[33] Diallo, D., Benbouzid, M. E. H., Hamad, D. & Pierre, X. Fault detection and diagnosis in an induction machine drive: A pattern recognition approach based on concordia stator mean current vector. *IEEE Transactions on Energy Conversion* **20**, 512–519 (2005).

[34] Gyftodimos, E. & Flach, P. A. Hierarchical bayesian networks: an approach to classification and learning for structured data 291–300 (2004).

[35] Allenby, G. M. & Rossi, P. E. Hierarchical bayes models. *The handbook of marketing research: Uses, misuses, and future advances* 418–440 (2006).

[36] Goodman, N. D. *et al.* Intuitive theories of mind: A rational approach to false belief **6** (2006).

[37] Fe-Fei, L. *et al.* A bayesian approach to unsupervised one-shot learning of object categories 1134–1141 (2003).

[38] Lee, C.-J. & Lee, K. J. Application of bayesian network to the probabilistic risk assessment of nuclear waste disposal. *Reliability Engineering & System Safety* **91**, 515–532 (2006).

[39] Eddine, A. H. Z., Zaarour, I., Guerin, F., Hijazi, A. & Lefebvre, D. Fault detection and isolation for zvs full bridge isolated buck converter based on observer design and bayesian network 344–349 (2011).

[40] Guérin, F. & Lefebvre, D. Adaptive generalized pid controllers and fuzzy logic coordinator for load sharing in smse 5588–5593 (2013).

[41] Colot, O., Olivier, C., Courtellemont, P., El-Matouat, A. & de Brucq, D. Information criteria and abrupt changes in probability laws. *Signal Processing VII: Theories and Applications* 1855–1858 (1994).

[42] Richards, F. S. A method of maximum-likelihood estimation. *Journal of the Royal Statistical Society Series B: Statistical Methodology* **23**, 469–475 (1961).